THz cavity ring-down quantitative gas phase spectroscopy

Coralie Elmaleh, Fabien Simon, Jean Decker, Julien Dumont, Fabrice Cazier, Marc Fourmentin, Robin Bocquet, A. Cuisset, Gaël Mouret, Francis Hindle

▶ **To cite this version:**

Coralie Elmaleh, Fabien Simon, Jean Decker, Julien Dumont, Fabrice Cazier, et al.. THz cavity ring-down quantitative gas phase spectroscopy. Talanta, 2023, 253, pp.124097. 10.1016/j.talanta.2022.124097 . hal-04013728

HAL Id: hal-04013728
https://ulco.hal.science/hal-04013728

Submitted on 16 Nov 2023

HAL is a multi-disciplinary open access archive for the deposit and dissemination of scientific research documents, whether they are published or not. The documents may come from teaching and research institutions in France or abroad, or from public or private research centers.

L'archive ouverte pluridisciplinaire **HAL**, est destinée au dépôt et à la diffusion de documents scientifiques de niveau recherche, publiés ou non, émanant des établissements d'enseignement et de recherche français ou étrangers, des laboratoires publics ou privés.

Distributed under a Creative Commons Attribution - NonCommercial - NoDerivatives 4.0 International License

Talanta 253 (2023) 124097

Contents lists available at ScienceDirect

Talanta

journal homepage: www.elsevier.com/locate/talanta

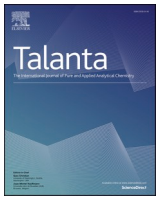

THz cavity ring-down quantitative gas phase spectroscopy

Coralie Elmaleh [a], Fabien Simon [a], Jean Decker [a,b], Julien Dumont [b], Fabrice Cazier [c], Marc Fourmentin [a], Robin Bocquet [a], Arnaud Cuisset [a], Gaël Mouret [a], Francis Hindle [a,*]

[a] Laboratoire de Physico-Chimie de L'Atmosphère, UR 4493, LPCA, Université du Littoral Côte d'Opale, 189A Av. Maurice Schumann, F-59140, Dunkerque, France
[b] Paprec Énergies 59, Pole de Valorisation Energétique, Rue Armand Carrel, 59140, Dunkerque, France
[c] Centre Commun de Mesures, Université du Littoral Côte d'Opale, F-59140, Dunkerque, France

ARTICLE INFO

Keywords:
Cavity ring-down spectroscopy
Terahertz spectroscopy
Trace gas
Air quality

ABSTRACT

The development of cavity based infrared spectroscopy techniques has proved very successful, in particular cavity ring-down spectroscopy for sensitive measurements. The construction difficulty of high finesse cavities has hindered the application of this approach for THz frequencies. We have successfully demonstrated finesse values of 3500 by using a corrugated waveguide and photonic mirrors. This cavity which is 48 cm in length provides an interaction length of 1 km. A quantitative measurement of the absorption of a gas sample introduced into the cavity is made by THz Cavity Ring-Down Spectroscopy and applied to several gases and samples. Firstly, a pure gas that weakly absorbs the radiation at this frequency show that line strengths of 10^{-27} cm^{-1}/(molecule.cm^{-2}) may be measured. A sub-ppm trace of HCN a particularly polar molecule with a strong THz signature has been examined and demonstrates a Limit Of Quantification (LOQ) of 3 ppb. Industrial samples extracted from a waste recovery facility have been measured and compared with a certified gas analyser. The results for SO_2, NO_2 and NO have been compared using the different techniques and show a good agreement.

1. Introduction

The frequency band from 100 GHz to 1 THz continues to attract the attention of a wide range of researchers in fields from astrophysics to security imaging. This is partially due to the promise of an excellent molecular discrimination but also because system components such as sources and detectors are becoming more easily available and with improved performance. Imaging systems operating at these frequencies are attractive as they are able to penetrate certain materials, amongst other examples this has led to full body scanners being deployed and tested for airport security screening [1]. The chemical analysis of an unknown gas phase sample is a sought-after application for which the THz band holds promise. Indeed, at low pressure the Doppler limited linewidths are particularly narrow allowing to resolve individual rotational transitions even in congested spectra and to unambiguously identify molecular signatures even in complex chemical mixtures. With such selectivity it is possible to discriminate molecules with close chemical structures such as isomers [2], conformers [3] or isotopomers, each of them having a unique rotational fingerprint. Direct quantification, without the requirement of any calibration standard, can be performed as the integrated absorption is related to the square of the permanent dipole moment of the molecule in question which is, experimentally and/or theoretically, well established [4]. This is not the case with the transition moments between rovibrational or rovibronic states, respectively in the IR and in the UV domains where absolute quantitative high-resolution spectroscopy is possible only with a small number of compounds listed in the atmospheric databases. At present only a small number of demonstrations of THz quantitative spectroscopy in different chemical mixtures can be found in the literature [5–9]. Nevertheless, the achievable instrument sensitivity presently limits the further development of such public or mass-market applications. If an increased sensitivity can be reliably obtained then a THz spectrometer should be able to provide a single instrument capable of measuring multiple chemical species with no interference between the rotational lines.

Astrophysics remains the most longstanding user of this waveband with several significant scientific programs having constructed high value instruments, for example the ALMA telescope [10], the HIFI instrument on the Herschel satellite [11], and the airborne GREAT spectrometer operated on the SOFIA platform [12]. It is also being employed

Abbreviations: CRDS, Cavity Ring-Down Spectroscopy; THz, Terahertz.

* Corresponding author.
E-mail address: francis.hindle@univ-littoral.fr (F. Hindle).

https://doi.org/10.1016/j.talanta.2022.124097
Received 17 October 2022; Received in revised form 8 November 2022; Accepted 9 November 2022
Available online 12 November 2022
0039-9140/© 2022 The Authors. Published by Elsevier B.V. This is an open access article under the CC BY-NC-ND license (http://creativecommons.org/licenses/by-nc-nd/4.0/).

to examine the earth's stratosphere [13,14]. The interpretation of the data obtained is strongly dependent on the availability of fundamental spectroscopic parameters which are measured by high-resolution spectroscopy laboratory-based studies. Examples range from the detailed absorption profiles measurements of small polar molecules with strong absorption signatures [15] to the probing weak absorptions of less abundant conformers in flexible molecules [3]. Once again, the sensitivity of the THz spectrometers used is a critical parameter determining the contours of the experimentally measurable dataset. Like the source power, and the detector noise, the path length of the interaction between the sample and propagating radiation strongly influences the spectrometer sensitivity. High-resolution studies of gases are commonly undertaken using a standard absorption configuration using a sample cell of around 1 m in length. The path length can be extended to a double-pass of even a multiple-pass configuration. Multiple-pass cells with base lengths varying from 50 cm to 5 m have yielded path lengths from around 20 to 200 m with improved sensitivity, they do suffer from a complex baseline and requirement of large sample volumes [16–19]. Further increases to the interaction length may be envisaged by replacing the multiple-pass cell by a resonant cavity. Initially developed by O'Keefe and Deacon [20] who coupled a pulsed laser to a cavity, measuring the absorption spectrum of the sample by Cavity Ring-Down Spectroscopy (CRDS). This topic was actively pursued to increase the achievable instrument sensitivity, which included the use of continuous-wave (cw) lasers for high resolution measurements by both CRDS and Cavity Enhanced Absorption Spectroscopy (CEAS) [21]. The rapid developments of these techniques in the infrared were possible due to the availability of high reflectivity spherical mirrors and relatively inexpensive, powerful, fibre coupled lasers diodes from telecommunications research. For example, commercially available mirrors with a reflectivity of 99.99% are available, with a 1 m cavity will result in a ring-down time of 33 μs and an equivalent interaction distance of 10 km.

In cw-CRDS the laser is coupled to the cavity which also acts as a measurement chamber. Once the power inside the cavity reaches a sufficient threshold level the laser source is rapidly extinguished, and the ring-down of the light trapped inside the cavity is observed by a sensitive detector outside the cavity [22]. A quantitative value of the absorption coefficient is directly determined from the value of the ring-down time with and without the gas-sample being present in the cavity. This approach has the advantage of being independent of the amplitude noise of the laser source. The difficulty is to match the laser to the cavity resonance which is much narrower than a free running laser. Several different strategies may be adopted, the simplest is to apply a modulation either to the laser frequency or the cavity length [23]. Provided that the modulation ensures an excursion corresponding to at least one free spectral range then the laser and cavity will be periodically matched to produce a ring-down event. Alternatively, actively locking the cavity and the laser together has yielded higher sensitivities due to higher and more reproducible intra-cavity powers, and an increased data accumulation rate [24]. The locking of lasers to high finesse cavities is however not straightforward, requires high bandwidth control loops, and significantly increases the complexity of the setup.

A simpler alternative that has proved popular is CEAS [25], where the cavity is continuously illuminated and the intensity of the transmitted light recorded. In this case no mechanism to rapidly extinguish the laser source is required. For this approach to be efficient, it is desirable to modify the cavity response to increase the number of modes. This can be done by partially misaligning the cavity and introducing mechanical instabilities. The signal that is recorded in CEAS is the intensity transmitted by the cavity with and without the absorbing molecule being present. To obtain a quantitative value of the absorption coefficient using CEAS the mirror reflectivity and cavity length must be well known, hence a calibration step is used [21]. Unlike CRDS, CEAS spectra are not directly quantitative, this represents the principal disadvantage of CEAS.

The construction of high finesse cavities for frequencies in the 0.1 to 1 THz range has proved challenging due to the lack of high-reflectivity spherical mirrors. Nevertheless cavities using wire grid polarisers for reflectors combined with an off-axis parabolic mirror to refocus the radiation have been tested [26,27]. The wires grid polarisers allow the source to be coupled to the cavity and also provide a small leakage signal that may be used for detection. Finesse values up to 350 have been demonstrated but remain insufficient to continue their development. Alternatively spherical silicon resonators have also been demonstrated, a whispering-gallery modes have been observed around 600 GHz but are limited to a finesse of 220 [28]. In this work we will use a new type of THz cavity composed of an oversized low loss corrugated waveguide and plane photonic mirrors achieving a finesse of 3500 at 620 GHz [29]. The existing measurements provide only a qualitative absorption signal using a CEAS configuration, here the THz cavity ring-down times have been measured for the first time yielding a quantitative determination of the absorption coefficient. With an equivalent interaction length of 1 km, we will demonstrate the use of this cavity for the first THz-CRDS measurements and the quantification gas samples.

2. Materials and methods

A THz cavity ring-down spectrometer was constructed using a continuous wave THz source, a cavity and a detection system. An Amplified Multiplier Chain (AMC) feed by a standard microwave synthesiser provided a frequency stable monochromatic source that may be readily modulated. The AMC (Virginia Diodes/Versys) with a multiplication factor of 54 generates a power level of −18 dBm (15 μW) at 600 GHz before launching the radiation into free space via a horn antenna. A quasi-optical setup with a polymethylpentene lens (f = 50 mm) was employed to couple the source to the THz cavity. Photonic mirrors were made by stacking a series of 4 high resistivity silicon discs (>10 kΩ cm) of 185 μm thickness separated by spacers ensuring gap of 375 μm between the discs. The optical thicknesses were selected to target a maximum of reflectivity around 600 GHz. The mirrors can be used from 565 to 635 GHz. The low-loss circular waveguide, 20.5 mm diameter and 48 cm in length, was electroformed copper with gold plating fabricated by Thomas Keating Company, having corrugations with a pitch of 166 μm and 125 μm deep to minimize losses around 600 GHz [30]. The complete cavity was formed by closing the waveguide with two photonic mirrors, as shown in Fig. 1. At the cavity exit, a second polymethylpentene lens (f = 50 mm) focused the radiation onto a zero-biased Schottky detector (Virginia Diodes/Versys).

Both mirrors could be finely moved by a piezo actuator to obtain the desired cavity length. The cavity assembly was placed in a gas chamber equipped with Teflon windows, pressure gauge, gas inlet and a turbo pump allowing a residual pressure less than 10^{-3} mbar to be achieved. At the output of the cavity the transmitted radiation was focused onto a zero-bias detector with a second polymethylpentene lens (f = 50 mm). The electrical signal was amplified by 60 dB before being sampled by a rapid data acquisition card containing an overhead-free averaging module (Spectrum Instruments). Unlike the infrared, in our case the cavity free spectral range is much larger than the Doppler limited molecular linewidth. For example, $FSR/\Delta\nu_{Doppler}$ is around 600 in our case and would fall to 0.6 for a 1 m cavity operating with a 1 μm wavelength source. Hence to probe the spectral profile of a molecular line, the AMC frequency and cavity mode should be simultaneously scanned over the region of interest. This was achieved by locking the cavity length to the AMC frequency. To facilitate the control loop, a Frequency Modulation (FM), typically of 100 kHz, was applied to the source. When detected at the modulation frequency, the centre of the cavity mode corresponds to a zero-crossing position, Fig. 1. A PID regulator was used to detect and lock the zero-crossing by applying a correction signal to a piezo actuator of one of the photonic mirrors. A robust lock was easily obtained and maintained as the AMC frequency was scanned. Pulses with a duration of 10 μs were injected into the cavity, while the data acquisition with a sampling rate of 1.25 GS/s was triggered at the end of the pulse. The

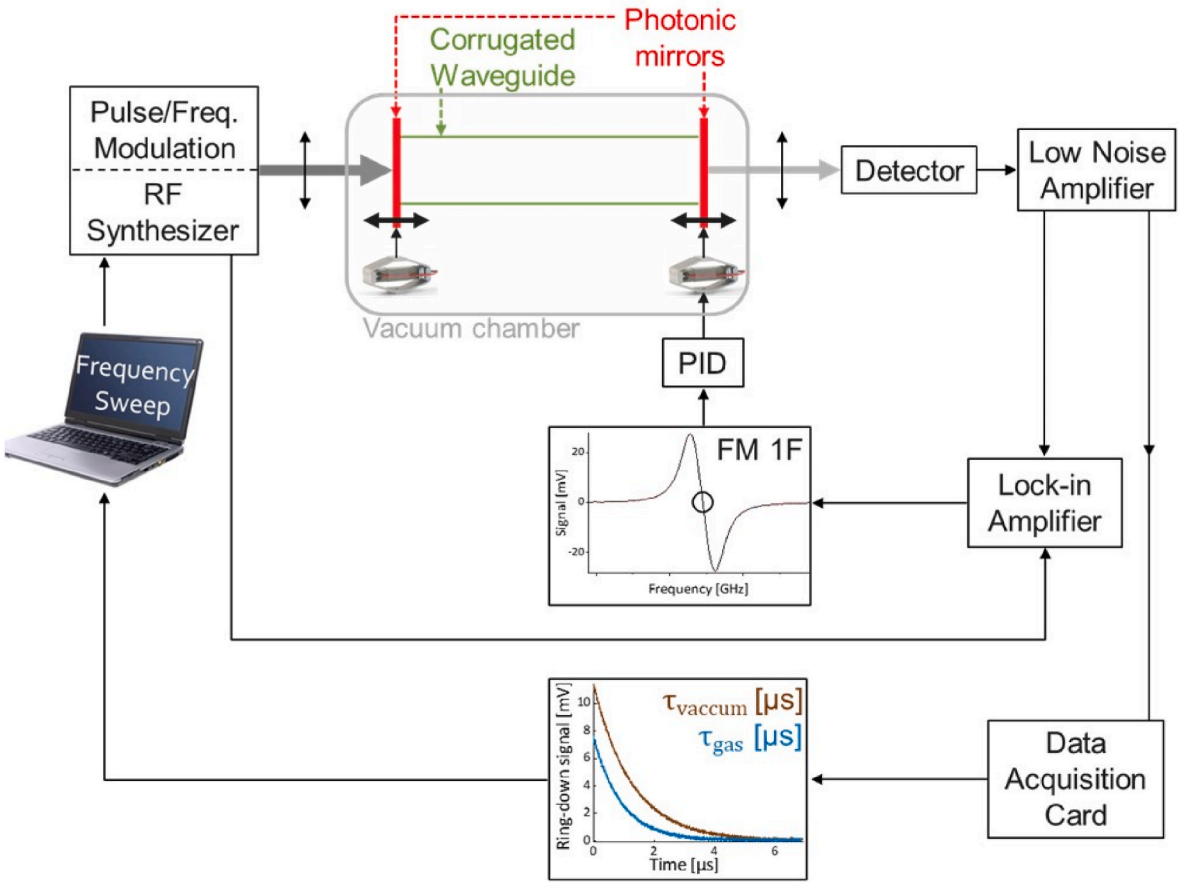

Fig. 1. THz cavity ring-down spectrometer. The emission of a microwave synthesiser and amplified multiplier chain is injected into the cavity. The ring-down signal is amplified by 60 dB with a bandwidth of 200 MHz. The DAQ samples and provides a real time average used to determine the ring-down time. The cavity length is locked to the emission frequency using piezo-electric actuators and a PID control loop.

stability of the cavity and the AMC frequency reliably allow the measurement of 5×10^4 ring-down events per second to be recorded. Their average waveform is calculated in real time by a dedicated acquisition card that can process up to 16×10^6 events. Examples of ring-down signals are given in Fig. 2 along with the response of the system without the cavity being present. Pure N_2O at 0.505 mbar was introduced into the measurement cell and the weak absorption of the $N_2^{18}O$ isotope probed at 617.727 GHz. A specifically written LabVIEW® (National Instruments) program was used to automate the control and data acquisition functions required for the operation of this instrument.

3. Results

Once the cavity is locked to the AMC frequency, a spectrum may be obtained by sweeping the frequency across the region of interest while the ring-down events are accumulated. The frequency stability of the AMC source allows the rapid accumulation of typically 10^5 ring-down events for each frequency point. The average waveform for a given data point provided by the acquisition card is automatically fitted with a standard exponential function by the LabVIEW® program. The complete spectrum of the ring-down time as a function of frequency is constructed point-by-point in this way.

3.1. Quantitative measurement of weak rotation lines

A well-known molecule was sought to access the sensitivity of the instrument, it is of particular importance that the line strengths are accurately known as they are required for the quantification of the absorbing species. Here we probe the J = 25 ← 24, pure rotation transition of N_2O in the $|v_1 = 1>$ vibrational state at room temperature. This transition, centred at 622.579 GHz, with a tabulated line intensity of 6.58×10^{-27} cm^{-1}/(molecule.cm^{-2}) [31], was selected to demonstrate the capacity of THz-CRDS to quantify weakly absorbing molecules. The instrument response was examined by recording the spectra of N_2O at various pressures, as shown in Fig. 3.

In order to conserve the molecular discrimination, the linewidths were kept close to the Doppler limit by restricting the maximum pressure to 3 mbar. A total of 19 spectra were recorded in the pressure range of 0.1–3 mbar. For each spectrum the baseline is recorded with an empty cavity under identical conditions. These spectra were all recorded using the average 10^5 ring-down events per data point, with a step size of 100 kHz. They typically contain 180 points requiring an acquisition time of approximately 6 min. The left-hand inset of Fig. 3 shows an example of the measured ring-down times τ with the gas present, and τ_0 without. The quantitative absorption coefficient α is directly obtained without the need to have either the exact length of the cavity or the finesse [22].

$$\alpha(\upsilon) = \frac{1}{c}\left(\frac{1}{\tau(\nu)} - \frac{1}{\tau_0(\nu)}\right) \quad (1)$$

The measured absorption coefficient shows a peak value of 5.5×10^{-7} cm^{-1} at the expected frequency for this transition. The data were fitted to a Voigt profile to account for both the Doppler and collisional line broadening. The line centre frequency and Doppler width were fixed to their expected values. The integrated line area from the minimised fit of each spectrum was used to determine the line transition intensity. The average line intensity evaluated from 19 spectra was 6.69×10^{-27} cm^{-1}/(molecule.cm^{-2}) with a standard deviation of 0.54×10^{-27} cm^{-1}/(molecule.cm^{-2}) refining the tabulated intensity value of 6.58×10^{-27}

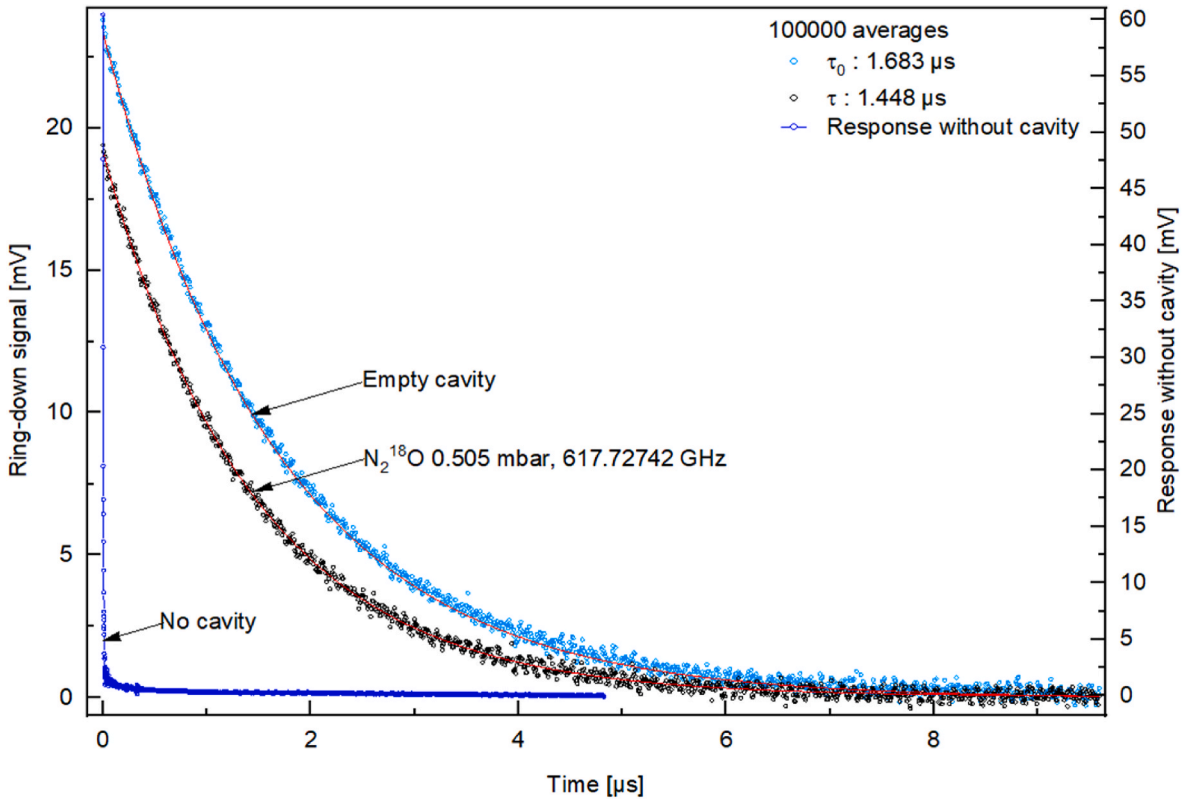

Fig. 2. Typical ring-down signals each obtained from 10^5 measured waveforms at 617.72742 GHz corresponding to the rotational line centre of the J = 26 ← 25 in $|v_2 = 1, l_2 = 1>$ excited state transition of $N_2^{18}O$. Light blue points for an empty cavity ($\tau_0 = 1.683 \pm 0.001$ µs) and black points with $N_2^{18}O$ in the cavity at a pressure of 0.505 mbar ($\tau = 1.448 \pm 0.001$ µs). For display purposes only one in every 10 points are displayed. The response of the detection system is illustrated by the waveform acquired without the cavity being present, dark blue points. (For interpretation of the references to colour in this figure legend, the reader is referred to the Web version of this article.)

$cm^{-1}/(molecule.cm^{-2})$. To further approach the sensitivity limit, a weaker rotational line of the $N_2^{18}O$ isotope (natural abundance of 2×10^{-3}) centred at 617.990 GHz was measured. This line shown in the right-hand inset of Fig. 3 corresponds to the J = 26 ← 25 rotational transition in the $|v_2 = 2, l = 2>$ excited state with an equivalent line strength estimated to be 1.88×10^{-27} $cm^{-1}/(molecule.cm^{-2})$ in a global fit with IR measurements [32,33]. This line is some 165,000 times weaker than the equivalent ground state transition of the most abundant isotope. THz-CRDS is intended for the quantitative measurement of weak absorbers, the presence of a strong absorption in the cavity will result in a non-exponential ring-down signals requiring a more complex interpretation [34].

3.2. Trace gas detection limit

In addition to measuring a weak line of a pure gas the system was used to measure a trace of a strongly absorbing molecule diluted in air or nitrogen. Hydrogen cyanide with a dipole moment of 2.984 D is a particularly strong absorber. When measuring a trace of 640 ppb of HCN diluted in nitrogen the molecular signal was observed to slowly decrease with time. We understand this to be caused by the adsorption of the HCN onto the metallic surface of the gas cell and waveguide. This is particularly important at low concentration levels and for the most polar molecules. This process was partially mitigated by flowing the gas through the sample cell rather than maintaining a static sample in a closed cell during the acquisition. When measuring a flow, the total pressure was obtained from the observed linewidth rather than from the static pressure gauge. A stable molecular signal was obtained, unfortunately at this particularly low pressure we were unable to quantify the flow using a commercially mass flow meter. The J = 7 ← 6 transition of the principal isotope of HCN, with a line strength of 2.52×10^{-19} $cm^{-1}/(molecule.cm^{-2})$, was measured at 620.304 GHz. The trace used was supplied by Messer and contained 640±19 ppb volume of HCN diluted in nitrogen, an example of the spectra obtained is given in Fig. 4.

In order to undertake the quantification of the HCN, the total pressure of the gas flow in the cavity should be known. Provided the line broadening coefficient is well know this can be determined using the observed collisional line width [35]. The data were fitted to a Voigt profile, initially the line centre frequency and Doppler width were fixed to their expected values, the signal to noise of the molecular signal was sufficient to allow these parameters to be freed once the collisional broadening and integrated line intensity were close to the final solution. A total pressure of 0.372 mbar was observed with a HCN concentration of 530±30 ppb. The principal source of uncertainty of this concentration measurement originates from the line broadening coefficient at 6% [35], the line strength is known with an uncertainty of 1% [36]. A small variation in the background during the scan is observed, we estimate the uncertainty due to this effect to be around 2%. The selectivity of the THz domain has allowed the $H^{13}CN$ to be observed, this isotope with a natural abundance of 1.1% presents an absorption some 83 times weaker than the principal isotope. In this case we consider that the observed variation in the ring-down time is close to the sensitivity limit for these averaging conditions, right-hand inset Fig. 4. Such a variation corresponds to a concentration of 8 ppb for the principal isotope.

3.3. Measurement of industrial samples

To further test the applicability of this instrument it was tested with industrial gas samples. At the present time the system is operated in a laboratory environment, although its deployment in an industrial setting

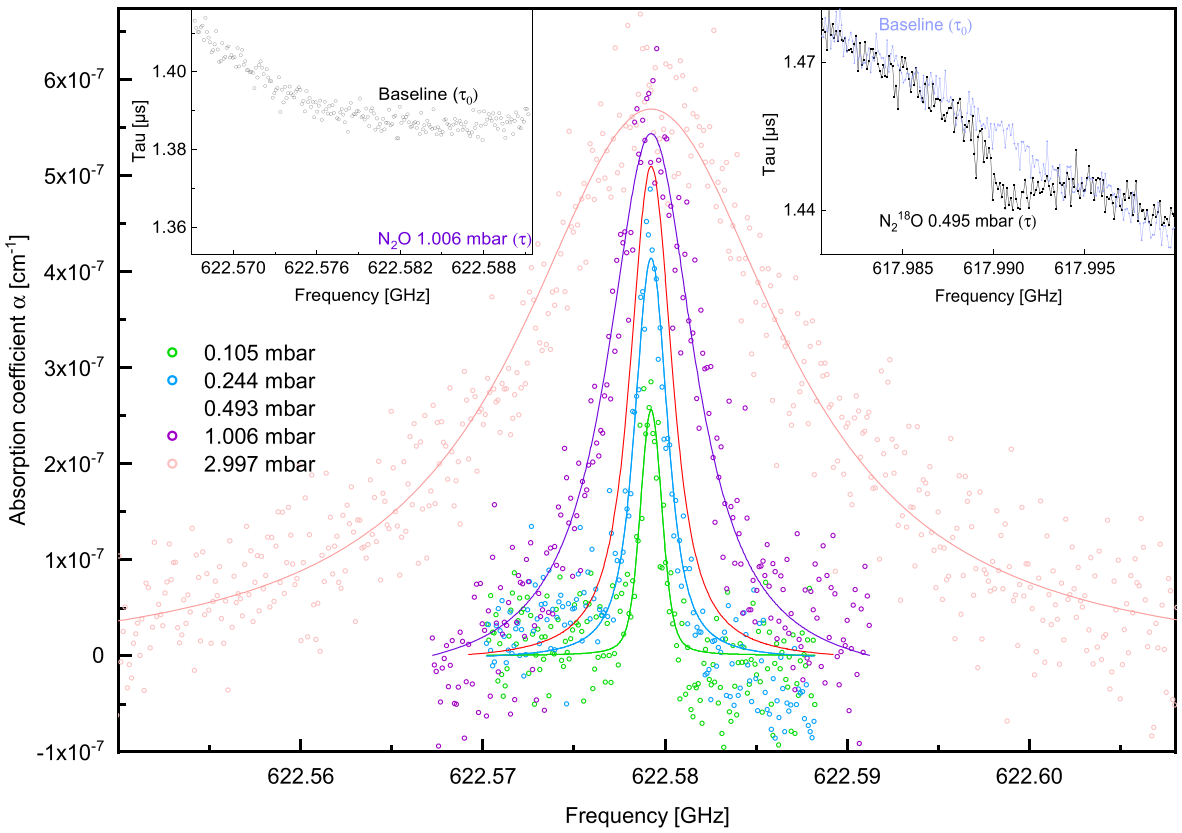

Fig. 3. Measured absorption coefficient for principal isotope of N_2O at 622.579 GHz ($J = 25 \leftarrow 24$ in $|v_1 = 1>$). Experimental data open round points, fitted Voigt profile solid lines. Left-hand inset, typical cavity ring-down time with gas and for an empty cavity. Right-hand inset measurement of the $N_2^{18}O$ isotope ($J = 26 \leftarrow 25$ in $|v_2 = 2, l = 2>$ excited state) having an abundance of 2×10^{-3}. All data taken for 10^5 ring-down events per point.

may be considered for on-line monitoring it was beyond the scope of this study. Gas samples were obtained from the energy recovery facility located in Dunkerque, France. This installation incinerates 250 tonnes of waste daily, recovering the thermal energy produced which covers the needs equivalent to approximately 17,000 households. The emissions of the incineration process are treated by an electro filter, a wet scrubber, and selective catalytic reduction before being monitored and released into the atmosphere. A small number of gas samples were available to demonstrate the potential of THz-CRDS to analyse industrial samples. A heated gas transfer line was used to extract gas samples from the emissions before the scrubber. A dedicated gas conditioning unit (M&C TechGroup, PSS5) was used to cool the sampled gas, typically at 165 °C, to 4 °C before filling multi-layer foil gas sampling bags. The samples were transported to the laboratory also located in Dunkerque and analysed the same day. Once THz-CRDS scan was completed the samples were immediately measured using a certified Portable Gas Analyser (PGA) (HORIBA PG-350EU). This analyser is also used *in-situ* verification of the sampling process. It uses cross flow measurements, using a non-dispersive infrared sensor for SO_2 and chemiluminescence for NOx, the latter being a Standard Reference Method (SRM). On site, an automated low resolution FTIR measurement system continuously monitors the regulated gas phase compounds (HCl, HF, CO, SO_2, NH_3, NO_x and Total Volatile Organic Compounds) before and after the gas treatment system. The measurement prior to treatment is used to control the process conditions of the gas treatment system. While the post treatment monitoring is required to satisfy the regulatory requirements for air quality. SO_2, NO_2 and NO were chosen among the regulated compounds, two values were obtained for SO_2, the second sample being taken 4 days after the first. The concentration of NO was determined using three overlapping transitions, a hyperfine structure originating from the nuclear quadrupole coupling of the nitrogen nucleus, modelled using three Voigt profiles. The concentration values for the THz-CRDS and PGA are given in Table 1 along with the line intensities.

3.4. Sensitivity limit

The sensitivity limit of the instrument is determined by our ability to measure the variation of the ring-down time. The available power and the transmission characteristics of the photonic mirrors leads to a weak signal at the cavity output that can be averaged over many ring-down events in order to improve the SNR. The experimental variation of the measured ring-down time for a given number of ring-down events was assessed by repeating the identical acquisition 10 times and taking the standard deviation. The values for up to 10^6 averages are shown in Fig. 5 for two different AMC sources. The standard AMC used in this study and specified to provide 15 μW, and a more powerful source (Lytid) covering a restricted spectral band but providing 1 mW. The standard deviation clearly decreases as the degree of averaging is increased as a function of the inverse square of the number of averages.

The smallest detectable value of the absorption coefficient can be calculated [37]:

$$\alpha_{\text{limit}} = \frac{\delta\tau}{c\tau_0^2\sqrt{N}} \tag{2}$$

where $\delta\tau$ is the uncertainty of the measurement of the ring-down time of a single event, N the number of events, and c the speed of light. The data show that $\delta\tau = 0.5$ μs for the standard AMC compared to $\delta\tau = 0.065$ μs for the higher power AMC.

4. Discussion

The combination of a low-loss corrugated waveguide and photonic

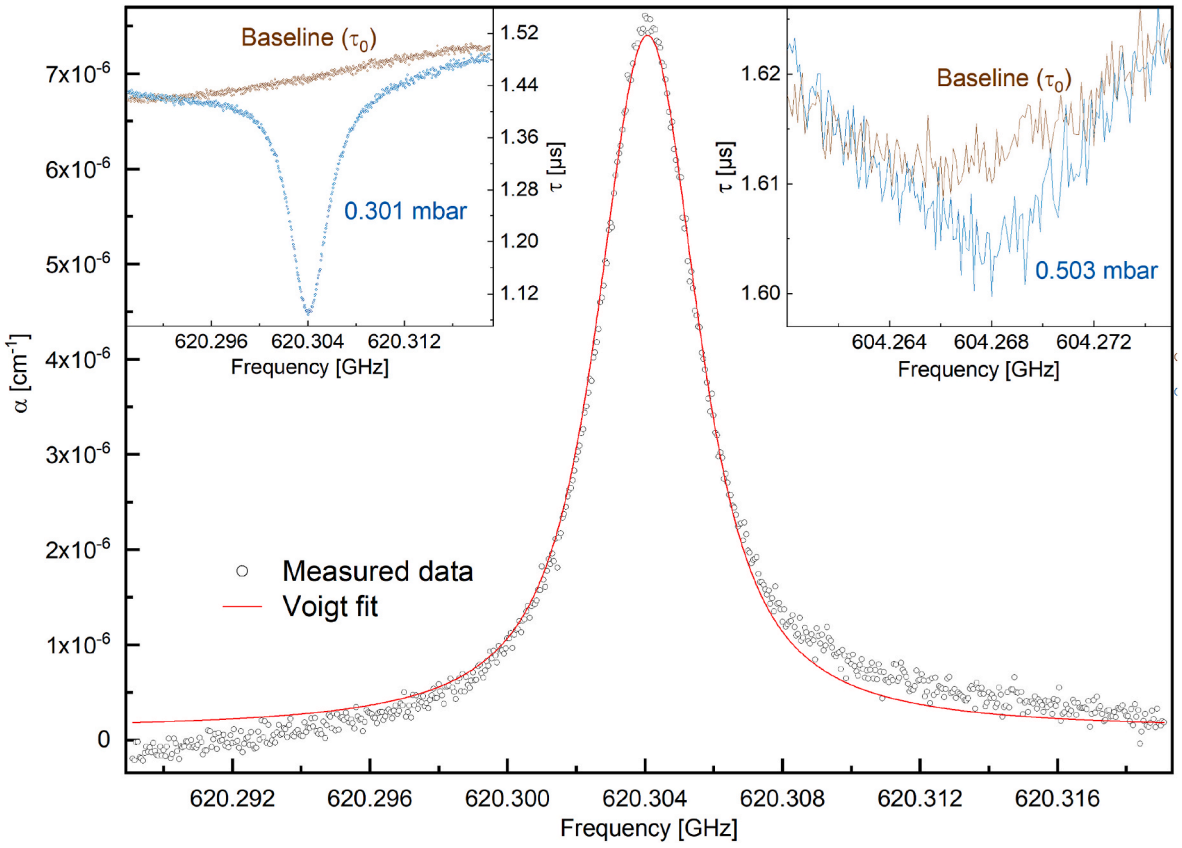

Fig. 4. Measured absorption coefficient for a 640 ppb trace of HCN, acquired using 10^5 ring-down waveforms per point. Experimental data open round black points, fitted Voigt profile red line. Left-hand inset, cavity ring-down time with trace gas and for an empty cavity, for the J = 7 ← 6 transition of the HCN principal isotope. Right-hand inset measurement of the $H^{13}CN$ isotope (natural abundance 1.1%), acquired using 3×10^5 ring-down waveforms per point. Pressure values shown correspond to those indicated by the static pressure gauge with the gas flow in the measurement cell. All measurements were performed at room temperature in an airconditioned laboratory. (For interpretation of the references to colour in this figure legend, the reader is referred to the Web version of this article.)

Table 1
Trace concentrations for several samples extracted before the wet scrubber of the energy recovery facility in Dunkerque.

Sample	N[a]	Trace species	Frequency GHz	Line intensity $cm^{-1}/(molecules.cm^{-2})$	Pressure[b] mbar	C_{CRDS} ppm	C_{PGA} ppm
1	5×10^4	SO_2	624.344	1.86×10^{-21}	0.42	30 ± 6	27.6 ± 0.9
2	5×10^4	SO_2	624.344	1.86×10^{-21}	0.38	87 ± 18	82 ± 2
2	10^5	NO_2	630.291	3.50×10^{-23}	0.35	90 ± 40	92 ± 3
3	10^5	NO	651.432 7	9.43×10^{-23}	0.38	31 ± 5	23.9 ± 0.7
			651.433 1	1.10×10^{-22}			
			651.433 6	8.05×10^{-23}			

[a] Number of ring-down events averaged per frequency point.
[b] Total pressure determined from observed linewidth.

mirrors have allowed weak absorption signals to be measured by THz-CRDS, which has the advantage of directly providing a quantitative value of the absorption coefficient. In the case of a pure gas the line intensities are reliably obtained and the observation of the $N_2^{18}O$ isotope indicates that the detection limit can be expected at 10^{-27} $cm^{-1}/(molecule.cm^{-2})$. This value corresponds to that found previously using CEAS [29] and is limited by the cavity losses and the available source power. Unlike CEAS, the THz-CRDS gives a quantitative value for the absorption coefficient. The measurement of pure gases does not suffer from adsorption, if some molecules adsorb onto the metallic surfaces the isotopic composition of the gas remains unchanged, and under static conditions a standard pressure gauge provides a reliable value for the total pressure. The measurement of trace gases is an attractive application of this technique nevertheless with the present system the sample gas is exposed to a large metallic surface. The strongest THz absorptions are displayed by highly polar molecules such as HCN, unfortunately they have a tendency to adsorb onto metallic surfaces modifying the trace concentrations levels of the gas mixture. This is of particular importance for low concentrations where the loss of a small quantity of molecules can easily exceed the required measurement uncertainty. Using a gas flow rather than a static sample we have measured a concentration of HCN of 530±30 ppb using the THz-CRDS compared to the expected 640 ppb, the difference is attributed to the adsorption losses. To overcome this difficulty the metal components should be replaced glass or plastic counterparts. The observation of the $H^{13}CN$ displays a variation in the ring-down time of around 5 ns, under these conditions expected minimum observable variation is 2 ns or $\alpha_{limit} = 2 \times 10^{-8}$ cm^{-1}. Comparing this value to the peak absorption of $7 \times 10^{-6} cm^{-1}$ for a HCN concentration of 530 ppb and setting the Limit Of Quantification (LOQ) to twice α_{limit} leads to a LOQ of 3 ppb. This value for HCN and is coherent with the low SNR for the observed $H^{13}CN$ line. The stated uncertainty of 30 ppb is dominated by the uncertainty of 6% for the HCN broadening

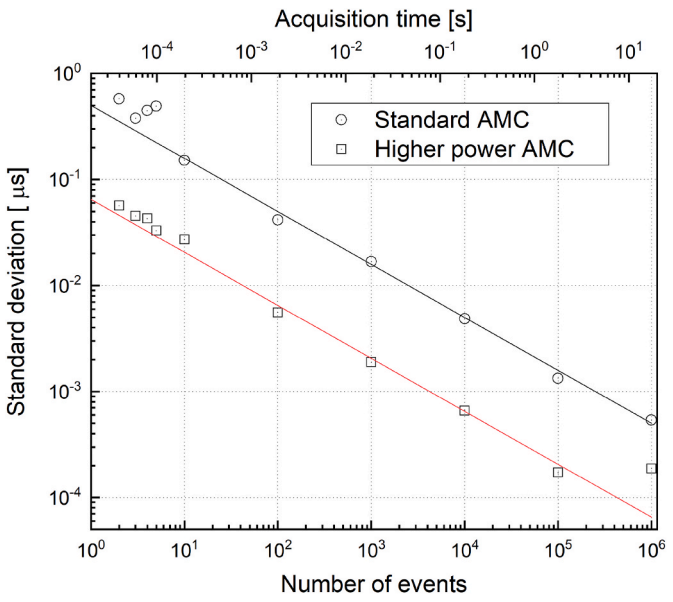

Fig. 5. Characterisation of the observed uncertainty of the cavity ring-down time as a function of the number of ring-down events averaged. Squares, standard AMC source. Circles, higher power AMC source. Solid lines model with expected variation dependent on $N^{-1/2}$. Recorded at 586.701 GHz.

coefficient used to determine the total pressure. It is critical to overcome the adsorption of the target molecule so that a static sample can be reliably measured and the full potential of this approach realised.

A small number of industrial gas samples, extracted prior to the wet scrubber of an energy recovery facility, were available. A few target molecules with weaker THz signatures than HCN have been quantified in the concentration range from 30 to 100 ppm. We notice that these measurements are less sensitive to adsorption problems as the target species less polar than HCN and the concentration levels are significantly higher. The agreement between the CRDS and the PGA quantification is excellent: better than 10% except for NO (25%) where the deconvolution of the rotational signature in 3 weakly intense components make the concentration determination difficult. THz CRDS enhances the capability of rotational spectroscopy to diagnostic complex chemical mixtures where numerous polar compounds may be monitored in gas phase at trace level with a single non-invasive technique. The concentration uncertainties were determined from those of the tabulated spectroscopic parameters (line intensity and air broadening coefficient) and the signal to noise of the molecular absorption. The uncertainty of the broadening coefficients is typically the dominate. Due to the smaller Doppler broadening compared to the infrared, the THz absorption lines are particularly narrow, typically with a full width half maximum around 5 MHz. This value is some 48,000 times finer than the resolution of the infrared Fourier transform spectrometer that continuously monitors the emissions of these targeted pollutants in the Dunkerque energy recovery facility. Rotational spectroscopy shows an exceptional degree of selectivity compared to the other spectroscopic techniques used for trace gas monitoring in complex chemical mixtures. In terms of detection limit the results obtained on SO_2, are coherent with the atmospheric emissions regulations, the daily emission limit value of which is less than 10 mg/m^3 or 3 ppm [38]. For NO_x, the daily emission limit value is 80 mg/m^3, corresponding to 35 ppm when measuring NO or 25 ppm when measuring NO_2, the LOQ on NO of about 5 ppm is sufficient but limiting for NO_2 with about 30 ppm.

5. Conclusion

The use of photonic mirrors and a corrugated waveguide have enabled the construction of a high-finesse cavity. For the first time THz CRDS has been demonstrated and has several advantages compared to its infrared counterparts. Firstly, the source is particularly stable in frequency and can be easily matched to a cavity mode. Once matched a simple control loop can be employed to lock the cavity to the source. The intensity of the radiation can be directly controlled by amplitude modulation of the microwave synthesiser feeding the AMC, hence the THz-CRDS is particularly simple. The measurement speed is only limited by the modulation pattern that is selected to allow suitable power build up in the cavity followed by the measurement of the ring-down time. An appealing advantage of THz spectroscopy is its selectivity due to particularly narrow linewidths. A single instrument can be used to measure several different chemical species as demonstrated here for HCN, N_2O, SO_2, NO_2, NO aswell as the $H^{13}CN$ and $N_2^{18}O$ minority isotopes. The sensitivity of the present instrument could be improved by increasing the power of the source or the transmission of the photonic mirrors used to couple the radiation into and out of the cavity. The adsorption of the target molecules onto the metallic surfaces of the cavity requires the use of a gas flow rather than a static sample. In this case the linewidth is used to determine the total pressure of the gas in the cavity. The accuracy achieved is limited by that of the broadening coefficient rather than the instrument sensitivity. We expect to overcome this removing, replacing or coating the metallic surfaces of the cavity and measurement cell.

Credits

Coralie Elmaleh: Validation, Investigation, Visualization, Writing—original draft preparation, Writing— review and editing **Fabien Simon:** Validation, Investigation **Jean Decker:** Validation, Investigation, Resources **Julien Dumont:** Resources **Fabrice Cazier:** Resources **Marc Fourmentin:** Software, Writing—original draft preparation **Robin Bocquet:** Conceptualization, Methodology **Arnaud Cuisset:** Validation, Writing—original draft preparation, Writing— review and editing, Supervison **Gaël Mouret:** Conceptualization, Methodology, Supervision, Project administration, Funding acquisition **Francis Hindle:** Conceptualization, Methodology, Software, Writing—original draft preparation, Writing— review and editing, Supervision, Project administration.

Declaration of competing interest

The authors declare the following financial interests/personal relationships which may be considered as potential competing interests: Gael Mouret reports financial support was provided by SATT Nord and and Labex CaPPA (Chemical and Physical Properties of the Atmosphere) funded by the French National Research Agency (ANR) through the PIA (Programme d'Investissements d'Avenir) under contract ANR-11-LABX-005-01. Gael Mouret has patent #WO/2019/002139 issued to SATT Nord.

Data availability

Data will be made available on request.

Acknowledgements

The authors would like to acknowledge the financial support of SATT Nord and Labex CaPPA (Chemical and Physical Properties of the Atmosphere) funded by the French National Research Agency (ANR) through the PIA (Programme d'Investissements d'Avenir) under contract ANR-11-LABX-005-01. The CIFRE PhD of Jean Decker is funded by the BIOGIE company in the context of the TERAWASTE project (CPER IRenE, phase 5) dedicated to determine the capabilities of THz spectroscopy to monitor the regulated emissions of a waste recovery centre.

References

[1] G. Tzydynzhapov, P. Gusikhin, V. Muravev, A. Dremin, Y. Nefyodov, I. Kukushkin, New real-time sub-terahertz security body scanner, J. Infrared, Millim. Terahertz Waves 41 (6) (2020) 632–641, https://doi.org/10.1007/s10762-020-00683-5. Jun.

[2] A. Roucou, M. Goubet, I. Kleiner, S. Bteich, A. Cuisset, Large amplitude torsions in nitrotoluene isomers studied by rotational spectroscopy and quantum chemistry calculations, ChemPhysChem 21 (22) (2020) 2523–2538, https://doi.org/10.1002/cphc.202000591. Nov.

[3] A. Roucou, et al., Full conformational landscape of 3-methoxyphenol revealed by room temperature mm-wave rotational spectroscopy supported by quantum chemical calculations, ChemPhysChem 19 (13) (2018) 1572–1578, https://doi.org/10.1002/cphc.201800148. Jul.

[4] S. Matton, et al., Terahertz spectroscopy applied to the measurement of strengths and self-broadening coefficients for high-J lines of OCS, J. Mol. Spectrosc. 239 (2) (2006) 182–189, https://doi.org/10.1016/j.jms.2006.07.004. Oct.

[5] D. Bigourd, et al., Detection and quantification of multiple molecular species in mainstream cigarette smoke by continuous-wave terahertz spectroscopy, Opt. Lett., OL 31 (15) (2006) 2356–2358, https://doi.org/10.1364/OL.31.002356. Aug.

[6] F. Hindle, et al., Monitoring of food spoilage by high resolution THz analysis, Analyst 143 (22) (2018) 5536–5544, https://doi.org/10.1039/C8AN01180J. Nov.

[7] C.F. Neese, I.R. Medvedev, G.M. Plummer, A.J. Frank, C.D. Ball, F.C.D. Lucia, Compact submillimeter/terahertz gas sensor with efficient gas collection, preconcentration, and ppt sensitivity, IEEE Sensor. J. 12 (8) (2012) 2565–2574, https://doi.org/10.1109/JSEN.2012.2195487. Aug.

[8] G. Mouret, et al., Versatile sub-THz spectrometer for trace gas analysis, IEEE Sensor. J. 13 (1) (2013) 133–138, https://doi.org/10.1109/JSEN.2012.2227055. Jan.

[9] N. Rothbart, et al., Millimeter-wave gas spectroscopy for breath analysis of COPD patients in comparison to GC-MS, J. Breath Res. 16 (4) (2022), https://doi.org/10.1088/1752-7163/ac77aa, 046001, Oct.

[10] A. Wootten, A.R. Thompson, The atacama large millimeter/submillimeter array, Proc. IEEE 97 (8) (2009) 1463–1471, https://doi.org/10.1109/JPROC.2009.2020572. Aug.

[11] T. de Graauw, et al., The herschel-heterodyne instrument for the far-infrared (HIFI), A&A 518 (2010) L6, https://doi.org/10.1051/0004-6361/201014698. Jul.

[12] S. Heyminck, U.U. Graf, R. Güsten, J. Stutzki, H.W. Hübers, P. Hartogh, GREAT: the SOFIA high-frequency heterodyne instrument, A&A 542 (2012) L1, https://doi.org/10.1051/0004-6361/201218811. Jun.

[13] L. Froidevaux, et al., Early validation analyses of atmospheric profiles from EOS MLS on the aura Satellite, IEEE Trans. Geosci. Rem. Sens. 44 (5) (2006) 1106–1121, https://doi.org/10.1109/TGRS.2006.864366. May.

[14] W. Wang, Z. Wang, Y. Duan, Performance evaluation of THz atmospheric limb sounder (TALIS) of China, Atmos. Meas. Tech. 13 (1) (2020) 13–38, https://doi.org/10.5194/amt-13-13-2020. Jan.

[15] M. Mouelhi, et al., Self and N2 broadening coefficients of H2S probed by submillimeter spectroscopy: comparison with IR measurements and semi-classical calculations, J. Quant. Spectrosc. Radiat. Transf. 247 (2020), 106955, https://doi.org/10.1016/j.jqsrt.2020.106955. May.

[16] J.S. Melinger, Y. Yang, M. Mandehgar, D. Grischkowsky, THz detection of small molecule vapors in the atmospheric transmission windows, Opt. Express, OE 20 (6) (2012) 6788–6807, https://doi.org/10.1364/OE.20.006788. Mar.

[17] J. Decker, et al., MULTICHARME: a modified Chernin-type multi-pass cell designed for IR and THz long-path absorption measurements in the CHARME atmospheric simulation chamber, Atmos. Meas. Tech. Discuss. (2021) 1–22, https://doi.org/10.5194/amt-2021-399. Dec.

[18] V. Boudon, O. Pirali, P. Roy, J.-B. Brubach, L. Manceron, J. Vander Auwera, The high-resolution far-infrared spectrum of methane at the SOLEIL synchrotron, J. Quant. Spectrosc. Radiat. Transf. 111 (9) (2010) 1117–1129, https://doi.org/10.1016/j.jqsrt.2010.02.006. Jun.

[19] A. Cuisset, et al., Terahertz rotational spectroscopy of greenhouse gases using long interaction path-lengths, Appl. Sci. 11 (3) (2021), https://doi.org/10.3390/app11031229. Art. no. 3, Jan.

[20] A. O'Keefe, D.A.G. Deacon, Cavity ring-down optical spectrometer for absorption measurements using pulsed laser sources, Rev. Sci. Instrum. 59 (12) (1988) 2544–2551, https://doi.org/10.1063/1.1139895. Dec.

[21] M. Mazurenka, A.J. Orr-Ewing, R. Peverall, G.A.D. Ritchie, 4 Cavity ring-down and cavity enhanced spectroscopy using diode lasers, 0, Annu. Rep. Prog. Chem., Sect. C: Phys. Chem. 101 (2005) 100–142, https://doi.org/10.1039/B408909J. Oct..

[22] J.H. van Helden, R. Peverall, G.A.D. Ritchie, Cavity enhanced techniques using continuous wave lasers, in: Cavity Ring-Down Spectroscopy: Techniques and Applications, 2010, pp. 27–56, https://doi.org/10.1002/9781444308259.ch2.

[23] D. Romanini, A.A. Kachanov, N. Sadeghi, F. Stoeckel, CW cavity ring down spectroscopy, Chem. Phys. Lett. 264 (3) (1997) 316–322, https://doi.org/10.1016/S0009-2614(96)01351-6. Jan.

[24] N.J. van Leeuwen, J.C. Diettrich, A.C. Wilson, Periodically locked continuous-wave cavity ringdown spectroscopy, Appl. Opt., AO 42 (18) (2003) 3670–3677, https://doi.org/10.1364/AO.42.003670. Jun.

[25] M.-C. Chan, S.-H. Yeung, High-resolution cavity enhanced absorption spectroscopy using phase-sensitive detection, Chem. Phys. Lett. 373 (1) (2003) 100–108, https://doi.org/10.1016/S0009-2614(03)00540-2. May.

[26] B. Alligood DePrince, B.E. Rocher, A.M. Carroll, S.L. Widicus Weaver, Extending high-finesse cavity techniques to the far-infrared, Rev. Sci. Instrum. 84 (7) (2013), https://doi.org/10.1063/1.4813274, 075107, Jul.

[27] R. Braakman, G.A. Blake, Principles and promise of Fabry–Perot resonators at terahertz frequencies, J. Appl. Phys. 109 (6) (2011), https://doi.org/10.1063/1.3560771, 063102, Mar.

[28] D.W. Vogt, R. Leonhardt, Ultra-high Q terahertz whispering-gallery modes in a silicon resonator, APL Photon. 3 (5) (2018), https://doi.org/10.1063/1.5010364, 051702, Feb.

[29] F. Hindle, R. Bocquet, A. Pienkina, A. Cuisset, G. Mouret, Terahertz gas phase spectroscopy using a high-finesse Fabry–Pérot cavity, Optica 6 (12) (2019) 1449, https://doi.org/10.1364/OPTICA.6.001449. Dec.

[30] E.J. Kowalski, et al., Linearly polarized modes of a corrugated metallic waveguide, IEEE Trans. Microw. Theor. Tech. 58 (11) (2010) 2772–2780, https://doi.org/10.1109/TMTT.2010.2078972. Nov.

[31] W.-J. Ting, et al., Precision frequency measurement of N2O transitions near 4.5 μm and above 150 μm, J. Opt. Soc. Am. B, JOSAB 31 (8) (2014) 1954–1963, https://doi.org/10.1364/JOSAB.31.001954. Aug.

[32] I. E. Gordon et al., 'The HITRAN2020 molecular spectroscopic database', J. Quant. Spectrosc. Radiat. Transf., vol. 277, 2022, doi: 10.1016/j.jqsrt.2021.107949.

[33] S.A. Tashkun, V.I. Perevalov, E.V. Karlovets, S. Kassi, A. Campargue, High sensitivity cavity ring down spectroscopy of N2O near 1.22 μm: (II) 14N216O line intensity modeling and global fit of 14N218O line positions, J. Quant. Spectrosc. Radiat. Transf. 176 (2016) 62–69, https://doi.org/10.1016/j.jqsrt.2016.02.020.

[34] I. Sadiek, G. Friedrichs, Saturation dynamics and working limits of saturated absorption cavity ringdown spectroscopy, Phys. Chem. Chem. Phys. 18 (33) (2016) 22978–22989, https://doi.org/10.1039/C6CP01966H. Aug.

[35] C. Yang, et al., Oxygen, nitrogen and air broadening of HCN spectral lines at terahertz frequencies, J. Quant. Spectrosc. Radiat. Transf. 109 (17–18) (2008) 2857–2868, https://doi.org/10.1016/j.jqsrt.2008.08.005.

[36] A. Maki, W. Quapp, S. Klee, G. Ch Mellau, S. Albert, The CN mode of HCN: a comparative study of the variation of the transition dipole and herman–wallis constants for seven isotopomers and the influence of vibration–rotation interaction, J. Mol. Spectrosc. 174 (2) (1995) 365–378, https://doi.org/10.1006/jmsp.1995.0008. Dec.

[37] Vincent Motto-Ros, 'Cavités de haute finesse pour la spectroscopie d'absorption haute sensibilité et haute précision : Application à l'étude de molécules d'intérêt atmosphérique', thesis, Université Claude Bernard - Lyon I, 2005.

[38] Joint Research Centre (European Commission), G. Cusano, S. Roudier, F. Neuwahl, S. Holbrook, J. Gómez Benavides, Best available techniques (BAT) reference document for waste incineration: industrial emissions directive 2010/75/EU (integrated pollution prevention and control), LU: Publications Office of the European Union Accessed: Oct. 10, 2022. [Online]. Available: https://data.europa.eu/doi/10.2760/761437, 2019.